Ngo Minh Khoa[1], Doan Duc Tung[1,*]

J. Electrical Systems 14-2 (2018): 192-204

Regular paper

An Extended Kalman Filter for Detecting Voltage Sag Events in Power Systems

Voltage sag event is one of the most important power quality disturbances in power systems. It can have affect on voltage quality and sensitive equipment in power systems. Detecting voltage sag events in power systems is a vital role in operating systems; therefore, this paper proposes an algorithm based on extended Kalman filter (EKF) for characterizing and detecting the parameters of voltage sag events accurately. A status-space modeling of voltage sag signals is defined to model voltage sag signal according to status-space modeling of EKF. The parameters of voltage sag events are estimated using the proposed method including voltage magnitude, estimation error, starting and ending times, duration time of the event. Matlab software is used to generate database of voltage sag waveforms modeled by a mathematical equation and then the waveforms are used to evaluate the proposed method. The simulation results of the proposed method are also compared with the simulation results of the root mean square (RMS) method to confirm the effectiveness of the proposed method in this paper.

Keywords: Voltage sag; Kalman filter; Gaussian noise; power quality disturbances; power system.

Article history: Received: 09 March 2018, Accepted: 9 May 2018

1. Introduction

Nowadays, industrial customers use more and more electronic devices such as frequency converter, inverter, rectifier, etc. to improve the efficiency of work and bring economic benefit. However, these devices are very sensitive to power quality disturbances such as harmonics, sag, swell, transients, overvoltage, etc. [1]-[4], [8]. Among these, voltage sag event is a type of power quality disturbance which is the most common and important in power systems. Moreover, voltage sag events are very harmful to sensitive equiment because they can have affect on the operation mode of many electrical devices at the point of common coupling. Voltage sag is a phenomenon that the voltage magnitude decreseases over a short period of time and is caused by short circuit problems, sudden increase in load, starting up large asynchronous motor, etc. [6]. Therein, the most common cause of voltage sag is short circuit in power systems. Short circuits on transmission lines or distribution lines have an affect on a large number of electrical customers. Short circuits on transmission lines affect sensitive electrical equipment that can range up to hundreds of kilometers far away the location of fault [5, 6].

There are many methods to detect voltage sag in power systems. Methods such as RMS method, peak voltage method, memory voltage method [7, 11], etc. are traditional methods. They are simple and easy to implement but they have limits in the detection and estimation of magnitude and duration of voltage sag events. In [7], short-time Fourier transforms is applied to detect and characterize the voltage events in power systems. The results show that the accuracy of this method depends on the selected window length. Wavelet transform

[*] Corresponding author: Doan Duc Tung, Faculty of Engineering and Technology, Quy Nhon University, 170 An Duong Vuong Street, Quy Nhon city, Binh Dinh province, Vietnam, E-mail: doanductung@qnu.edu.vn

[1] Faculty of Engineering and Technology, Quy Nhon University, Vietnam

is a powerful signal processing tool for analyzing nonstationary signals. Discrete wavelet transform has been successfully applied to monitor the power quality disturbances in power systems [7, 9, 10]. The main disadvantage of wavelet transform, however, is that it depends on the selected mother wavelet, analysis level, and sensitivity to noise. Other modern methods are also used to analyze power quality disturbances such as Hilbert transform, Gabor transform, Gabor-Wigner transform, S transform, and Hilbert-Haung transform, but each method has its own advantages and disadvantages as analyzed in [8], [20]-[22].

Recently, there are several papers published about the dection and classification of power quality disturbances. The authors in [24] proposed a new method for detection and classification of single and combined power quality disturbances using a sparse signal decomposition on overcomplete hybrid dictionary matrix. The method in [24] can detect and classify single and combined PQ disturbances under noiseless and noisy conditions. The M-band Wavelet packet transform had been made to analyze power quality disturbances in [25]. The reference [26] also presented a technique for automated power quality disturbance detection and classification in power distribution system using cross-correlation-based approach in conjunction with fuzzy logic. The method requires minimum number of features when compared with conventional approaches for identification of power quality disturbances. A hybrid approach to classify power quality disturbances by using support vector machine, discrete wavelet transform, and discrete Fourier transform was proposed in [27] to extract features from a good number of actual measured PQ events occurred in a transmission system.

For the purpose of quickly and accurately detecting voltage sag events, EKF has many advantages over other methods. Because it can accurately determine voltage sag magnitude, starting and ending times of the event [7], [12]-[19], [23]. Moreover, EKF do not depend on other characteristics of voltage sag such as point on wave, phase jump angle, sag shape, etc. In this paper, the authors propose a method based on extended Kalman filter for detecting voltage sag events. The highlight of the proposed method in this paper is simple and implement easily. In addition, a status-space modeling based on papameters of voltage sag signals is defined to model voltage sag signal according to status-space modeling of EKF. Then the parameters of voltage sag signals are included in the modeling are determined by the EKF.

The rest of this paper is organized as follows. The background of modelling of voltage sag signal, the RMS method and the algorithm of the proposed method based on EKF are explained in Section 2. In Section 3, simulation results are shown and are discussed in detail in order to evaluate the method proposed in Section 2. The comparision between of simulation results of proposed method and the RMS method is clearly presented in Section 3. Finally, the conclusion is included in Section 4.

2. Methods analysis

2.1. The modeling of voltage sag signal

The modelling of voltage sag signals is an important task in detecting their parameters accurately. Voltage sag and swell waveforms are generally shown in Figure 1(a). The times at which the voltage waveform starts and ends shifting are called the starting (t_1) and ending time (t_2) of event, respectively. Depending on the starting time of event (t_1), the voltage sag will have different shapes. The difference between the starting time of event (t_1) and previous crossing by zero is called the point on wave. In Figure 1(a), the starting time of event (t_1) coincides with previous crossing by zero; therefore, the point on wave of the events is 0^0. The voltage magnitude decreases in the duration as shown in Figure 1(b).

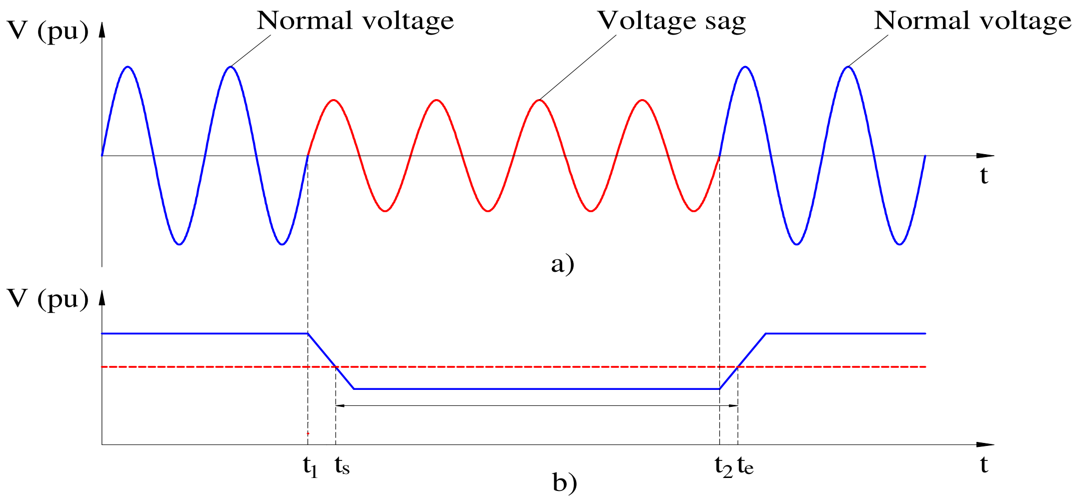

Figure 1. Voltage sag event: a) Waveform; b) Magnitude.

In general, a voltage sag signal can be defined as a periodic nonsinusoidal volage waveform which can be written an infinite sum of harmonics as follows [7]:

$$v(n) = V_0 + \sum_{h=1}^{\infty} \sqrt{2} V_h \cos\left(h\omega n T_s - \alpha_h\right) \tag{1}$$

where: $v_1(n) = \sqrt{2} V_1 \cos\left(\omega n T_s\right)$ (2)

is referred to the fundamental component of the voltage or simply the fundamental voltage with the RMS voltage V_1. The phase angle of the fundamental voltage is taken as zero without any loss of generality. The term is as follows [7]:

$$v_h(n) = \sqrt{2} V_h \cos\left(h\omega n T_s - \alpha_h\right) \tag{3}$$

is referred to the harmonic h of the h^{th} harmonic component of the voltage; V_h is the RMS value of harmonic h; a_h is its phase angle with reference to the fundamental voltage. Note that there is no unique way to define the phase-angle difference between sine waves of different frequency [7].

2.2. The RMS method

From the sampled voltages, one or more characteristics as a function of time are calculated for every recording. Most sensors use the RMS voltage as a function of time as the only event characteristic. This function is used to determine the retained voltage and the duration of the event [11, 16, 17]. The RMS voltage is calculated over a one-cycle interval and is updated every half cycle.

To calculate the RMS voltage, the sampled voltages are squared and averaged over a window with a one-cycle duration [6, 7], as in (4):

$$V_{rms(1/2)}(n) = \sqrt{\frac{1}{N} \sum_{i=1+n-N}^{n} v_i^2} \tag{4}$$

where N is the number of samples per cycle.
v_i is the sampled voltage waveform.
n is 1, 2, 3, etc.

The sampling should be synchronized to the power frequency. That is, the sampling frequency is not a fixed number of samples per second but a fixed number of samples per cycle. This synchronization to the power frequency (also referred to as "phase-locked-loop") is essential for the quantification of harmonic distortion and phase angle change calculations. For RMS voltage, the difference between synchronized and nonsynchronized measurements is small [6].

2.3. The proposed method based on EKF

Kalman filters addressed so far in this section are designed to estimate the state vector in a linear system model. The reference [13] proposed an adaptive Kalman filter for the voltage sag detection. In the paper, the state covariance matrix is changed through the simulation to enhance the Kalman filter in order to detect the amplitude changing of the fundamental component. Howerver the voltage sag signal in [13] is assumed that it is linear model and its fundamental frequency is constant. Morever, the voltage sag signals simulated in the reference [13] are noiseless. In fact, the underlying system model is nonlinear; therefore, we need to apply the EKF through a linearization procedure in this paper [7]. Instead of state-space modeling of linear systems, nonlinear systems are modeled by the following two sets of equations.

State equations: $\boldsymbol{x}(n+1) = \boldsymbol{f}(\boldsymbol{x}(n), n) + \boldsymbol{w}(n)$ (5)

Observation equations: $\boldsymbol{z}(n) = \boldsymbol{h}(\boldsymbol{x}(n), n) + \boldsymbol{v}(n)$ (6)

To obtain a linear system, we assume that there exists a (local/global) nominal state trajectory $\overline{\boldsymbol{x}}(n)$ and a (local/global) nominal output trajectory $\overline{z}(n)$ and let the deviations be denoted by

$$\begin{aligned} \delta\boldsymbol{x}(n) &= \boldsymbol{x}(n) - \overline{\boldsymbol{x}}(n) \\ \delta z(n) &= z(n) - \overline{z}(n) \end{aligned} \tag{7}$$

Recalling the Taylor series expansion of a function $f(y)$ in a neighborhood of $y = y_0$

$$\begin{aligned} f(y) = f(y_0) + f'(y_0)(y - y_0) + \frac{1}{2} f''(y_0)(y - y_0)^2 + \cdots \\ + \frac{1}{n!} f^{(n)}(y_0)(y - y_0)^n + e_n(y) \end{aligned} \tag{8}$$

Assuming that $\boldsymbol{x}(n)$ and $\boldsymbol{z}(n)$ are close to the nominal state and output trajectories, the state and observation equations can be approximated by Taylor series expansion of $\boldsymbol{f}$ and

$\boldsymbol{h}$ in a neighborhood about nominal values. Linear approximation can be obtained by retaining up to the first-order terms in the Taylor series expansion [7].

For the state and the observation equations in (6), this approximation yields the following state-space modeling:

$$\begin{aligned} \delta\boldsymbol{x}(n+1) &= \boldsymbol{A}_n \delta\boldsymbol{x}(n) + \boldsymbol{w}(n) \\ \delta z(n+1) &= \boldsymbol{C}_n \delta\boldsymbol{x}(n) + \boldsymbol{v}(n) \end{aligned} \tag{9}$$

where $\boldsymbol{A}_n$ and $\boldsymbol{C}_n$ are the Jacobian matrices of $\boldsymbol{f}$ and $\boldsymbol{h}$, defined as:

$$\boldsymbol{A}_n = \left.\frac{\partial \boldsymbol{f}\left(\boldsymbol{x}(n), n\right)}{\partial \boldsymbol{x}}\right|_{\boldsymbol{x}=\overline{\boldsymbol{x}}} = \begin{bmatrix} \dfrac{\partial f_1}{\partial x_1} & \cdots & \dfrac{\partial f_1}{\partial x_N} \\ \vdots & \ddots & \vdots \\ \dfrac{\partial f_N}{\partial x_1} & \cdots & \dfrac{\partial f_N}{\partial x_N} \end{bmatrix} \tag{10}$$

$$\boldsymbol{C}_n = \left.\frac{\partial \boldsymbol{h}\left(\boldsymbol{x}(n), n\right)}{\partial \boldsymbol{x}}\right|_{\boldsymbol{x}=\overline{\boldsymbol{x}}} = \begin{bmatrix} \dfrac{\partial h_1}{\partial x_1} & \cdots & \dfrac{\partial h_1}{\partial x_N} \\ \vdots & \ddots & \vdots \\ \dfrac{\partial h_N}{\partial x_1} & \cdots & \dfrac{\partial h_N}{\partial x_N} \end{bmatrix} \tag{11}$$

In order to estimate voltage sag parameters, a vector of status variables $\boldsymbol{x}(n)(4\times 4)$ is defined as (12) for modelling a nonlinear system.

$$\boldsymbol{x}(n) = \begin{bmatrix} x_1(n) \\ x_2(n) \\ x_3(n) \\ x_4(n) \end{bmatrix} = \begin{bmatrix} \theta(n) \\ \omega(n) \\ V_m(n) \\ \varphi(n) \end{bmatrix} \tag{12}$$

where: $\theta(n) = n\omega(n)T_s$.

Because the sampling time is very small so the voltage change can be ignored, the frequency and phase angle between two constitute samples. Therefore, we can estabilish the following equation:

$$\begin{aligned} \omega(n+1) &= \omega(n) \\ V_m(n+1) &= V_m(n) \\ \varphi(n+1) &= \varphi(n) \end{aligned} \tag{13}$$

From (12) and (13), we assume that noise is omitted in the state-space modeling, we can express the relationship between state vectors $\boldsymbol{x}(n+1)$ and $\boldsymbol{x}(n)$ as follows:

$$\begin{bmatrix} \theta(n+1) \\ \omega(n+1) \\ V_m(n+1) \\ \varphi(n+1) \end{bmatrix} - \begin{bmatrix} \theta(n) \\ \omega(n) \\ V_m(n) \\ \varphi(n) \end{bmatrix} = \begin{bmatrix} (n+1)\omega(n)T_s \\ \omega(n+1) \\ V_m(n+1) \\ \varphi(n+1) \end{bmatrix} - \begin{bmatrix} n\omega(n)T_s \\ \omega(n) \\ V_m(n) \\ \varphi(n) \end{bmatrix} = \begin{bmatrix} \omega(n)T_s \\ 0 \\ 0 \\ 0 \end{bmatrix} \tag{14}$$

This implies:

$$\begin{bmatrix} \theta(n+1) \\ \omega(n+1) \\ V_m(n+1) \\ \varphi(n+1) \end{bmatrix} = \begin{bmatrix} \theta(n)+\omega(n)T_s \\ \omega(n) \\ V_m(n) \\ \varphi(n) \end{bmatrix} = \begin{bmatrix} 1 & T_s & 0 & 0 \\ 0 & 1 & 0 & 0 \\ 0 & 0 & 1 & 0 \\ 0 & 0 & 0 & 1 \end{bmatrix} \begin{bmatrix} \theta(n) \\ \omega(n) \\ V_m(n) \\ \varphi(n) \end{bmatrix} \tag{15}$$

In fact, noise always exists in the state-space modelling; therefore, the equation (15) could be written simply arcoding to (5) as follows:

$$\boldsymbol{x}(n+1) = \boldsymbol{f}\left(\boldsymbol{x}(n), n\right) + \boldsymbol{w}(n) \tag{16}$$

where: $\boldsymbol{w}(n)$ is the vector of noise which is assumed as a Gaussian noise with covariance matrix $E\{\boldsymbol{w}(n)\boldsymbol{w}^T(n)\} = \boldsymbol{Q}_w$;

We can see that (16) have the same format of (6); therefore, we can determine the function $\boldsymbol{h}(\boldsymbol{x}(n), n)$ in (6) as follows:

$$h\left(\boldsymbol{x}(n), n\right) = V_m(n)\sin\left(n\omega(n)T_s + \varphi(n)\right) = x_3(n)\sin\left(x_1(n) + x_4(n)\right) \tag{17}$$

From (10) and (17) we get the matrix $\boldsymbol{A}_n$:

$$\boldsymbol{A}_n = \left.\frac{\partial \boldsymbol{f}\left(\boldsymbol{x}(n), n\right)}{\partial \boldsymbol{x}}\right|_{\boldsymbol{x}=\overline{\boldsymbol{x}}} = \begin{bmatrix} 1 & T_s & 0 & 0 \\ 0 & 1 & 0 & 0 \\ 0 & 0 & 1 & 0 \\ 0 & 0 & 0 & 1 \end{bmatrix} \tag{18}$$

From (11) and (17), this implies $\boldsymbol{C}_n$:

$$\boldsymbol{C}_n = \left.\frac{\partial \boldsymbol{h}\left(\boldsymbol{x}(n), n\right)}{\partial \boldsymbol{x}}\right|_{\boldsymbol{x}=\overline{\boldsymbol{x}}} = \begin{bmatrix} x_3(n)\cos\left(x_1(n) + x_4(n)\right) \\ 0 \\ \sin\left(x_1(n) + x_4(n)\right) \\ x_3(n)\cos\left(x_1(n) + x_4(n)\right) \end{bmatrix}^T \tag{19}$$

Thus after using the hypotheses and transforms, the voltage sag signals could be expressed by a space-state modeling including a set of state equations (5) and observation equations (6). Therefore, we can apply the proposed method based on EKF for this modeling in order to estimate parameters of voltage sag/sell signals including: magnitude V_m, phase angle φ.

Figure 2 shows the algorithm of the proposed method based on EKF to estimate parameters of voltage sag events.

3. Simulation results and discussion

To evaluate the proposed method as mentioned in Section 2, this section uses the voltage sag waveforms by using a mathematics equation that shows all voltage sag parameters as follows [10]:

$$v(t) = \begin{cases} V_m \sin(\omega t) & If \quad t < t_1 \\ V_{sag} \sin(\omega t + \varphi) & If \quad t_1 \le t \le t_2 \\ V_m \sin(\omega t) & If \quad t > t_2 \end{cases} \tag{20}$$

where: V_m - the voltage magnitude before and after occurring a voltage sag event;
ω - The frequency in radian;
V_{sag} - the voltage magnitude durring the duration of voltage sag event;
φ - The phase angle;
t_1 - The starting time of the voltage sag;
t_2 - The ending time of the voltage sag;
$\Delta t = t_2 - t_1$: The duration of the voltage sag.

Voltage sag waveforms generated according to (20) using Matlab software have voltage sag magnitude of 0.5 pu and a duration of cycles (0.1 sec). It assumes that the voltage magnitude before and after the voltage sag is equal to 1.0 pu and the total time of the voltage waveform is simulated for a period of 10 cycles (0.2 sec). Moreover, the voltage signals can be accompanied by noise, so this paper studies the voltage sag signals added noise with different levels of signal-to-noise ratio (SNR) to evaluate the proposed method. Two cases are investigated in this paper as follows:

Case 1 : *Voltage sag without noise.*

A 0.5 pu voltage sag waveform which occurs in a duration of 5.0 cycles (0.1 sec) is shown in Figure 3(a). Applying the proposed method mentioned in Section 2 to analyze the waveform, the simulation results including estimation error as shown in Figure 3(b). The signal in Figure 3(b) is the error between the actual voltage sag signal and the estimation voltage signal by the proposed method. The estimation error result shows clearly the starting and ending time of the voltage sag event. There are large error values because of the sudden change in the voltage signal at these times. As a result of the state variables of the proposed method, the magnitude of the votlage sag is shown in Figure 3(c). In particular, the voltage magnitude estimated from the proposed method was compared with the voltage magnitude determined from the RMS method. The simulation results show that the proposed method detects voltage sag accurately.

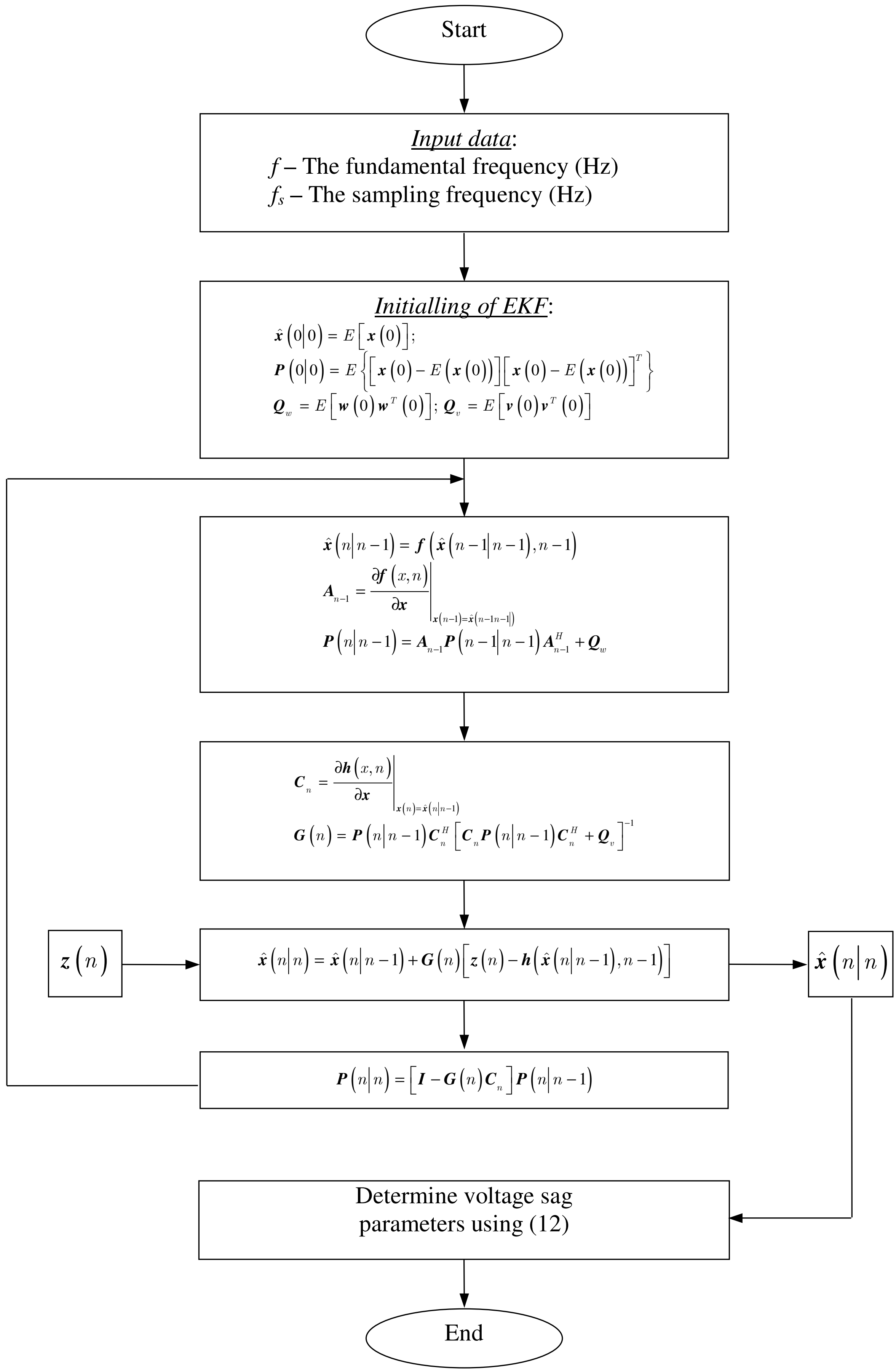

Figure 2. The algorithm of the proposed method.

Case 2 : *Voltage sag with Gausian noise.*

In fact, the actual voltage waveforms may be accompanied by noise; therefore, in order to evaluate the effectiveness of the proposed method in the detection of voltage sag waveforms with noise, this paper assumes that white Gaussian noise with three SNR levels including: SNR = 40 dB, SNR = 30 dB, and SNR = 20 dB will be added to the initial voltage sag waveform. The voltage sag waveforms with three SNR levels of noise are shown in Figure 4(a), Figure 5(a), and Figure 6(a), respectively. Depending on the SNR level of noise, the estimation error values of the proposed method are different as shown in Figure 4(b), Figure 5(b), and Figure 6(b), respectively. The voltage magnitudes of the voltage sag waveforms with three SNR levels of noise which are also determined using the proposed method and the RMS method are shown in Figure 4(c), Figure 5(c), and Figure 6(c), respectively. Although the voltage sag waveform is added noise, the proposed method still accurately determines the magnitude of the voltage sag and the simulation result is also compared to the simulation result of the RMS method.

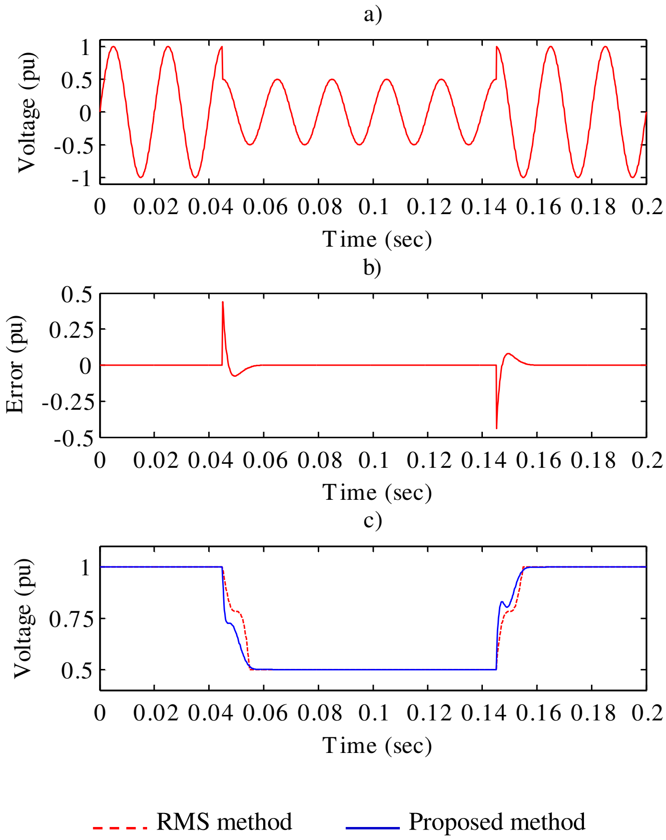

Figure 3. Case 1: a) Voltage waveform; b) Estimation error; c) Magnitude.

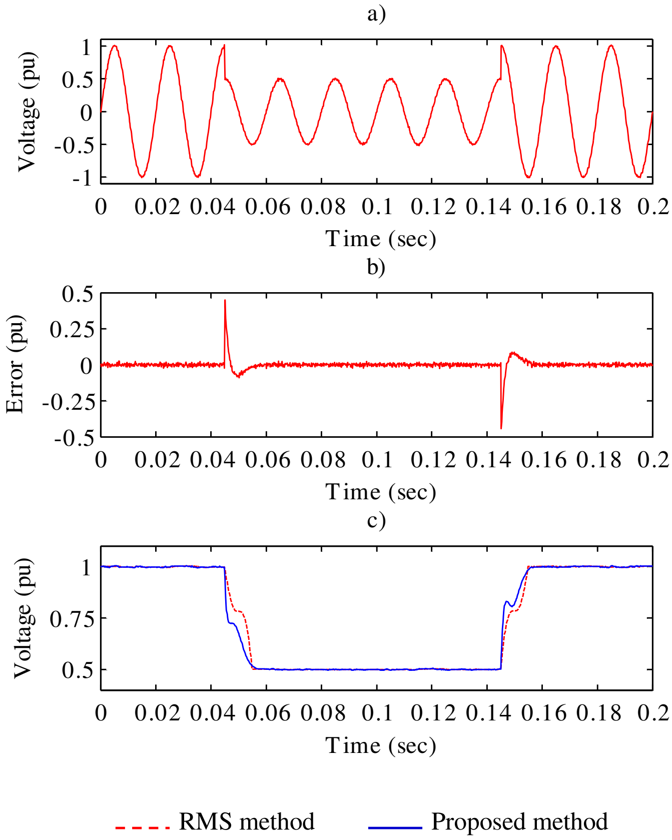

Figure 4. Case 2 (SNR = 40 dB); a) Voltage waveform; b) Estimation error; c) Magnitude.

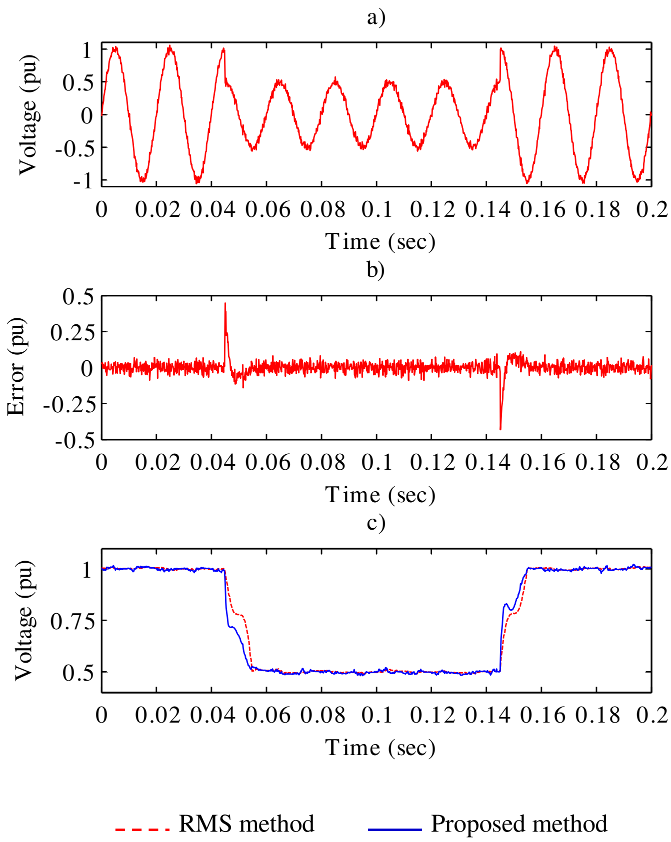

Figure 5. Case 2 (SNR = 30 dB); a) Voltage waveform; b) Estimation error; c) Magnitude.

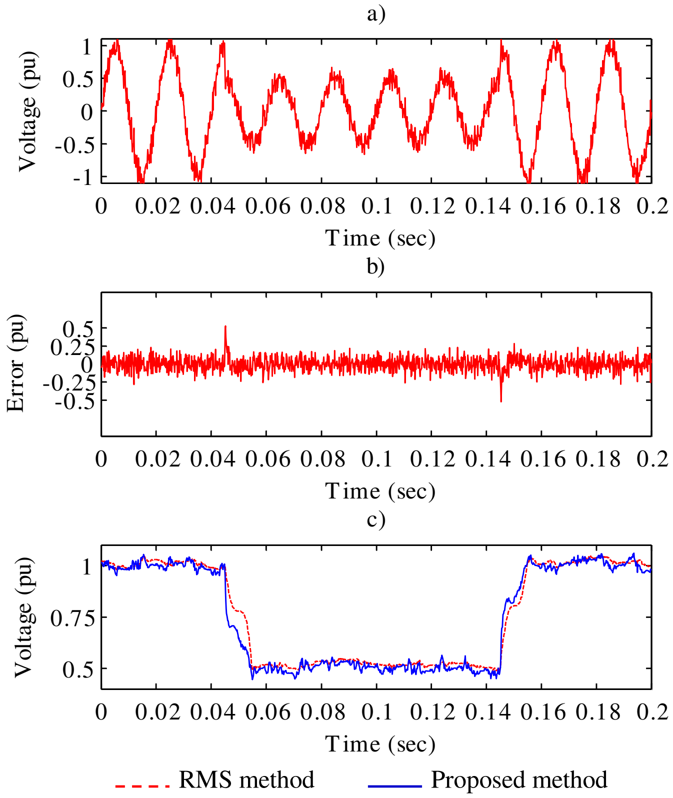

Figure 6. Case 2 (SNR = 20 dB); a) Voltage waveform; b) Estimation error; c) Magnitude.

The aforementioned voltage sag/swell waveforms are studied for both cases of varying their magnitude and the point on wave in order to evaluate the effectiveness of the proposed method. The voltage sag waveforms with duration of 5.0 cycles (0.1 sec) have magnitudes varying from 0.1; 0.2; 0.3;...; 0.9 pu and the point on wave varying from 0^0; 45^0; 90^0;...; 360^0. Then the proposed method is applied to determine the duration of the waveforms. The 3D plot results are shown in Figure 7. Simulation results show that the parameters of voltage sag waveform such as the magnitude, point on wave, etc. also have affect on the ability to determine the starting and ending times of the voltage sag event. In addition, the noise is also an external factor that we need to pre-process before applying the method proposed in this paper.

4. Conclusion

On the background of EKF method, this paper studied the modeling of voltage sag signals which consists of 4 variables which can express the charateristic of the state-space modeling of EKF method. Then, an algorithm based on EKF method is proposed for detecting the parameters of voltage sag events. The results obtained from the proposed method are the magnitude, the starting time, and the ending time of voltage sag event. This paper also analyzed and evaluated the effectiveness of the proposed method based on voltage sag signals which are modeled by mathematical equations. The results of the proposed method are also compared with the RMS method to confirm the effectiveness of the proposed method. In addition, Gaussian noise with three SNR levels is added to the voltage sag waveforms in order to test and evaluate the proposed method for detecting voltage sag events in condition with noise. The simulation results show that the proposed method detect voltage sag event accurately in both cases of with and without noise.

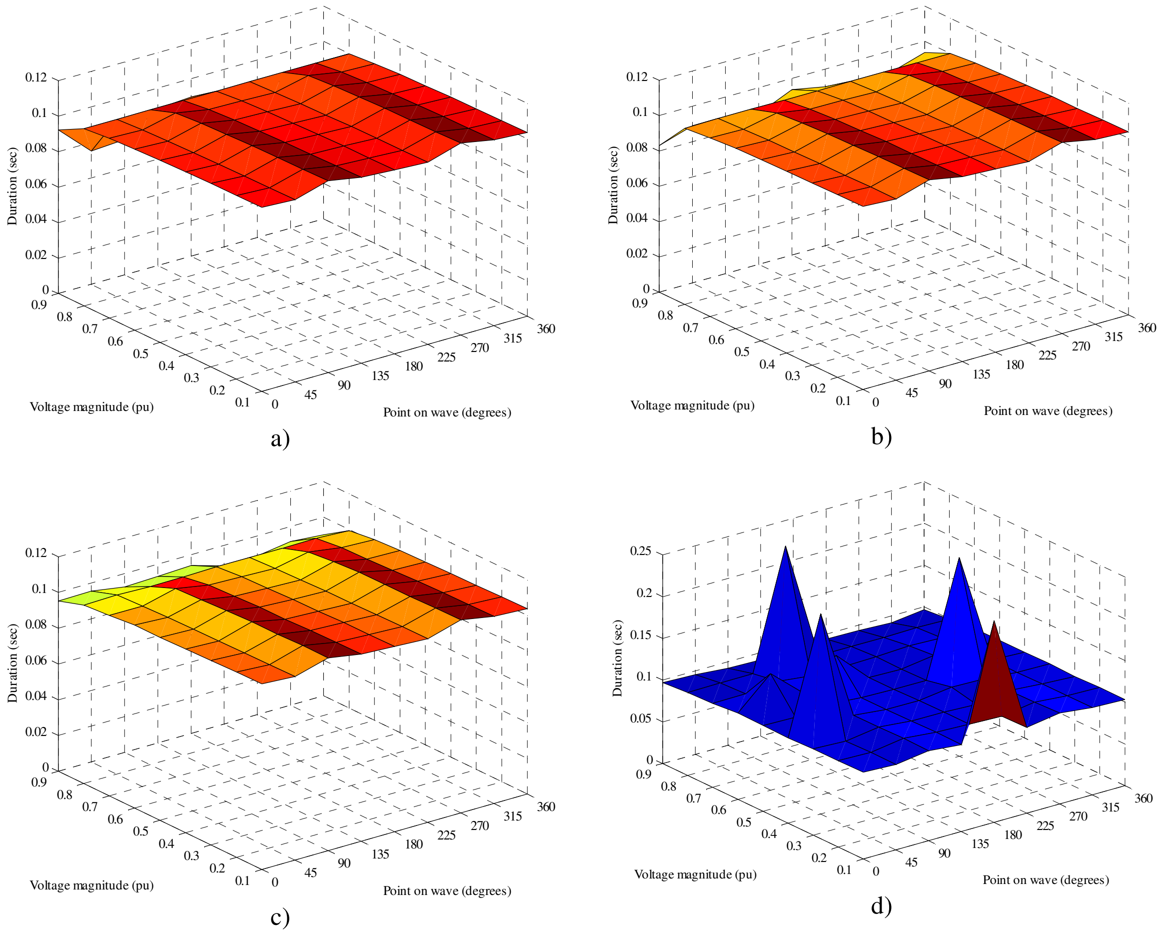

Figure 7. The duration of voltage sag events using the proposed method; a) Sag events without noise; b) Sag events with Gaussian noise (SNR = 40 dB); c) Sag events with Gaussian noise (SNR = 30 dB); d) Sag events with Gaussian noise (SNR = 20 dB).

Acknowledgment

The authors gratefully acknowledge the support of Quy Nhon University for the financial support. We are also thankful to Faculty of Engineering and Technology, Quy Nhon University for their encouragement and technical support to carry out this work.

References

[1] M. M. Zaid, M. U. Malik, et al. Detection and classification of short and long duration disturbances in power system, *Journal of Electrical Systems, 13*(4), 779-789, 2017.

[2] C. Venkatesh, D. V. S. S. Siva Sarma, M. Sydulu, Dynamic voltage sag/swell compensator for industrial distribution system, *Journal of Electrical Systems, 6*(4), 530-547, 2010.

[3] M. R. Garousi, M. R. Shakarami, F. Namdari, Detection and classification of power quality disturbances using parallel neural networks based on discrete wavelet transform, *Journal of Electrical Systems*, *12*(1), 158-173, 2016.

[4] M. M. Savrun, A. Tan, T. Köroglu, et al. DSP controlled voltage disturbance generator, *Journal of Electrical Systems*, *14*(1), 174-187, 2018.

[5] S. Chandrashekhar Reddy, P. V. N. Prasad, A. Jaya Laxmi, Hybrid approach for voltage sag mitigation in distribution system by optimal location and size of distributed generation, *Journal of Electrical Systems*, *9*(2), 150-166, 2013.

[6] M. H. J. Bollen, *Understanding power quality problems: Voltage sags and interruptions*, New York: IEEE Press, Vol. 1, 2000.

[7] Math H. J. Bollen, Irene Yu-Hua Gu, *Signal processing of power quality disturbances*, Wiley-Interscience, IEEE Press, 2006.
[8] D. Saxena, K. Verma, S. Singh, Power quality event classification: an overview and key issues, *International Journal of Engineering, Science and Technology, 2*(3), 186-199, 2010.
[9] Ngo Minh Khoa, Dinh Thanh Viet, Nguyen Huu Hieu, Classification of power quality disturbances using wavelet transform and K-nearest neighbor classifier, *2013 IEEE International Symposium on Industrial Electronics (ISIE)*, Taipei, 1-4, Taiwan, May 2013.
[10] Dinh Thanh Viet, Nguyen Huu Hieu, Ngo Minh Khoa, A method for monitoring voltage disturbances based on discrete wavelet transform and adaptive linear neural network, *International Review of Electrical Engineering*, *11*(3), 314-322, 2016.
[11] E. Styvaktakis, M. H. J. Bollen and I. Y. H. Gu, Automatic classification of power system events using rms voltage measurements, *2002 IEEE Power Engineering Society Summer Meeting*, *2*, 824-829, 2002.
[12] M. Janabali, S. Meshksar, et al. Voltage sag state estimation for power distribution systems using Kalman filter, *IEEE International Symposium on Industrial Electronics*, 2449-2453, 2007.
[13] H. Alrawashdeh, J. Asumadu, Adaptive Kalman filter for voltage sag detection in power system, *IEEE Jordan Conference on Applied Electrical Engineering and Computing Technologies (AEECT)*, 1-6, 2013.
[14] M. A. Mostafa, Kalman filtering algorithm for electric power quality analysis: harmonics and voltage sags problems, *Large Engineering Systems Conference on Power Engineering*, 159-165, 2007.
[15] A. Elnady, M. M. A. Salama, Unified approach for mitigating voltage sag and voltage flicker using the Dstatcom, *IEEE Transactions on Power Delivery*, *20*(2), 992-1000, 2005.
[16] M. Gonzalez, V. Cardenas, R. Alvarez, Detection of sags, swells, and interruptions using the digital rms method and Kalman filter with fast response, *32nd Annual Conference on IEEE Industrial Electronics*, 2249-2254, 2006.
[17] M. Gonzalez, V. Cardenas, R. Alvarez, A fast detection algorithm for sags, swells, and interruptions based on digital rms calculation and Kalman filtering, *10th IEEE International Power Electronics Congress*, 1-6, 2006.
[18] F. Molnar-Matei, C. Sorandaru, LabVIEW implementation of tracking filters for voltage dip detection, *2013 IEEE EUROCON*, 897-902, 2013.
[19] J. Barros, E. Perez, A combined wavelet – Kalman filtering scheme for automatic detection and analysis of voltage dips in power systems, *2005 IEEE Russia Power Tech*, 1-5, 2005.
[20] E. Styvaktakis, I. Y. H. Gu, M. H. J. Bollen, Voltage dip detection and power system transients, *Power Engineering Society Summer Meeting*, *1*, 683-688, 2001.
[21] H. Amaris, C. Alvarez, et al. Application of advanced signal processing methods for accurate detection of voltage dips, *13th International Conference on Harmonics and Quality of Power*, 1-6, 2008.
[22] A. Moschitta, P. Carbone, C. Muscas, Performance comparison of advanced techniques for voltage dip detection, *IEEE Transactions on Instrumentation and Measurement*, *61*(5), 1494-1502, 2012.
[23] Dinh Thanh Viet, Nguyen Huu Hieu, Nguyen Le Hoa, Ngo Minh Khoa, A control strategy for dynamic voltage restorer, *2015 IEEE 11th International Conference on Power Electronics and Drive Systems (PEDS)*, 1106-1110, 2015.
[24] H. Singh Rupal; K. Thakur Ankit; Soumya R. Mohanty; Nand Kishor, Detection and classification of power quality disturbances using signal processing techniques, *2017 IEEE PES Asia-Pacific Power and Energy Engineering Conference (APPEEC)*, 2017, pp. 1 – 6.
[25] Pashmi Kumawat; Naimish Zaveri; Dineshkumar Verma, Analysis of power quality disturbances using M-band wavelet packet transform, *2017 International Conference on Signal Processing and Communication (ICSPC)*, 2017, pp. 364 – 368.
[26] Subhra De; Sudipta Debnath, Real-time cross-correlation-based technique for detection and classification of power quality disturbances, *IET Generation, Transmission & Distribution*, 2018, Vol. 12, Iss. 3, pp. 688 – 695.
[27] P. C. Chang; G. W. Chang; M. H. Shih; Y. Y. Chen; Y. H. Hong; Y. K. Yeh, A hybrid approach for detection and classification of power quality disturbances, 2017 IEEE Power & Energy Society General Meeting, 2017, pp. 1 – 5.